

# Estimation of Long-Range Interaction in Coarse-Grained Rotational Isomeric State Polyethylene Chains on a High Coordination Lattice

Junhan Cho

Department of Polymer Science and Engineering, Dankook University, San-8 Hannam Yongsan, Seoul, 140–714 Korea

Wayne L. Mattice\*

Maurice Morton Institute of Polymer Science, University of Akron, Akron, Ohio 44325-3909

Received August 27, 1996; Revised Manuscript Received November 25, 1996<sup>®</sup>

**ABSTRACT:** A new Monte Carlo simulation on a coarse-grained tetrahedral lattice was recently developed for rotational isomeric state polyethylene chains. The short-range interaction was included by extending the classical statistical weight matrix. To describe the cohesive nature of realistic polyethylene systems, nonbonded long-range interaction was considered. The second virial coefficient  $B_2$  of two chains under an interparticle potential was suitably written in a discretized form to be analyzed for this new lattice. Utilizing the vanishing  $B_2$  of a  $\Theta$  chain was previously suggested for the estimation of interaction parameters representing several nearest neighbors. This approach was shown to be sufficient for treatment of dilute solutions, where long-range interactions are relatively infrequent. This study presents an alternative method of parameter estimation which is more appropriate for the bulk state, where long-range interactions are abundant. Interaction parameters were defined from an averaging procedure of the Mayer function in the expression of  $B_2$ . In the latter method, the widely used Lennard-Jones potential and associated parameters for the monomeric unit were used to calculate the average Mayer function. The estimated interaction parameters were used to simulate the average neighbor occupancy and the nonbonded energy per monomer. The nonbonded energy showed a minimum when it was plotted as a function of density. The latter method is considered better for the estimation of long-range interaction and yielded the density of minimum energy in a physically reasonable range. The calculated cohesive energy was shown to be close to the range defined by experiment.

## Introduction

Many phenomena in macromolecular systems, such as the equilibration of polymer melts and the folding of proteins, have large characteristic sizes and long relaxation times. New simulation methods are needed for such systems because of the infeasibility of fully atomistic simulation of their properties. Our approach is to discretize the phase space (lattice model) and utilize the fast integer algorithm for the most time-consuming part of the simulation. The overall simulation can be broken down into three steps: (1) rapid mapping of an atomistic model onto a high coordination lattice; (2) equilibration (or evolution in time) on the high coordination lattice, utilizing an integer algorithm (the long relaxation times, cited in the opening sentence, are dealt with during this step); (3) rapid "reverse mapping" of selected snapshots from the high coordination lattice back to a fully atomistic system in the continuum. When necessary, the reverse mapping can be followed by a rapid energy minimization using a complete force field appropriate for the fully atomistic model. Our concern in this article is with the construction of a long-range interaction that is suitable for use in the second step on the high coordination lattice.

Most of the lattice simulations so far have treated a polymer chain as a collection of renormalized Kuhn segments. The local behavior of the polymer chains is largely overlooked. We therefore search for a new on-lattice simulation which can provide detailed information on chain conformations. The conformational prop-

erties of polymer chains are well described by the rotational isomeric state (RIS) model.<sup>1,2</sup> The RIS polyethylene (PE) chain is the simplest one that can be a good starting material. Since the bond angle between three successive carbon atoms is approximately tetrahedral and the torsional angles in PE are separated by ca. 120 °C, a diamond lattice is a natural choice for the RIS PE chains, and also for the backbone of many other vinyl polymer chains.<sup>3–5</sup>

Recently we coarse-grained the original RIS PE chain to unite two  $-\text{CH}_2-$  units into one monomer.<sup>3,4</sup> This procedure causes us to take only every second lattice site of the diamond lattice. For this reason, this lattice is called the second-nearest-neighbor diamond (2nnd) lattice. The three-dimensional view of the 2nnd lattice is identical to that of the face-centered cubic lattice. However, its name (2nnd lattice) conveys more effectively the motivation for its use in the coarse-grained method. The chain movements are well defined by successive one bead moves to adjacent empty sites.

The 2nnd lattice simulation was carried out recently for a single PE chain.<sup>4</sup> The short-range interaction was first introduced to the linear 2nnd chain. The atomistic RIS formalism was extended by coarse graining the expanded classical statistical weight matrix. Each element in the coarse-grained, expanded statistical weight matrix accounts for the interdependence of two successive steps on the 2nnd lattice, which corresponds to a sequence of torsion angles at four consecutive C–C bonds in the usual RIS model for PE. The coarse-grained RIS PE chain was shown to have the proper mean-squared end-to-end distance, compared with the atomistic RIS PE chain. For the simulation of the bulk system of PE, it is necessary to include the long-range

<sup>®</sup> Abstract published in *Advance ACS Abstracts*, January 15, 1997.

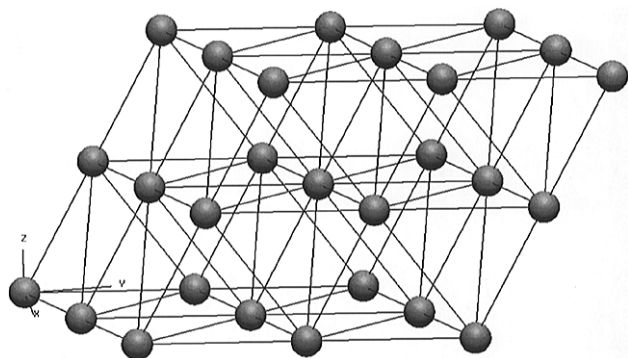


**Figure 1.** A part of the coarse-grained tetrahedral (2nd) lattice. This lattice can be viewed as a distorted cube. The cartesian  $x$ ,  $y$ , and  $z$  axes are shown in this figure. The corresponding  $\bar{x}$ ,  $\bar{y}$ , and  $\bar{z}$  axes of the 2nd lattice are distorted from the cartesian ones.

interaction between nonbonded monomers. It was suggested that reproducing the unperturbed dimension of a chain in a dilute solution in a  $\Theta$  solvent may be a way to extract the effective long-range interaction parameters.<sup>4,5</sup> As a first attempt, only two interaction parameters, for the first and second nearest shells, were included. The second virial coefficient  $B_2$  was suitably rewritten for the lattice system. Pairs of interaction parameters for the first and the second nearest shells were found using the requirement that  $B_2$  should vanish at the  $\Theta$  condition, using a simulation with a single chain.

The objective of this communication is to provide a different, simple method to estimate the long-range interaction parameters. This new method offers strong advantages in the simulation of amorphous systems a bulk density, as will be shown here. The basic idea is again to utilize the second virial coefficient. By comparing the discretized  $B_2$  for the (2nd) lattice with the  $B_2$  regenerated by a spherically symmetric potential for monomeric units, it may be possible to extract the interaction parameters via a suitable averaging procedure. In the next section, a detailed description of this procedure will be presented. In general, the inclusion of the long-range interaction extends the simulation length necessary for equilibration. There are, however, properties that equilibrate relatively quickly. Among these are the average occupancy of nearest neighbors and, therefore, the average energy per monomer. We test the suggested methods for long-range interaction by inspecting energy–density relations. Along with the density dependence of the long-range interaction energy, a cohesive energy can be easily calculated. This energy can also be compared with the experimental one for PE.

### Transformation of 2nd Lattice Coordinates to the Cartesian

It may be a prerequisite to understand the geometry of our 2nd lattice. As was briefly described, the 2nd lattice is obtained by skipping one lattice site out of every two sites on the diamond lattice. A part of the 2nd lattice is shown in Figure 1. The unit cell of the 2nd lattice can be seen as a distorted cube. The plane formed between two axes,  $\bar{x}$  and  $\bar{y}$  of the 2nd lattice, is a parallelepiped distorted by  $30^\circ$ . The angle between the 2nd  $\bar{z}$  axis and the Cartesian  $z$  axis is ca.  $35.25^\circ$ , since the C–C–C angle is ca.  $109.5^\circ$ . The transformation

equation between these two coordinate systems is therefore

$$\begin{bmatrix} x \\ y \\ z \end{bmatrix} = \begin{bmatrix} 1 & \cos 60^\circ & 1/\sqrt{3} \cos 30^\circ \\ 0 & \sin 60^\circ & 1/\sqrt{3} \sin 30^\circ \\ 0 & 0 & \sqrt{2}/\sqrt{3} \end{bmatrix} \begin{bmatrix} \bar{x} \\ \bar{y} \\ \bar{z} \end{bmatrix} \quad (1)$$

The 2nd lattice spacing for PE is  $2.5 \text{ \AA}$ , determined by the distance between next-nearest-neighbor carbon atoms when the bond length is  $1.53 \text{ \AA}$  and the bond angle is  $109.5^\circ$ .

### Definition of the Effective Interaction Parameters

The bulk properties of our model polymer system are determined by the choice of the interaction parameters between nonbonded mers on the 2nd lattice. Therefore it is of great importance to carefully select proper parameters. Let us reduce this problem to the simplest level. Consider that there are only two independent monomers in the system. This is a limiting case when the degree of polymerization goes to 1 and the number of chains in the system goes to 2. Parameters for nonbonded interaction may then be equated to parameters representing the interaction between one monomer at the origin and another in the specified 2nd lattice cell. A spherically symmetric potential  $u(r)$  is acting between these two monomers. According to the imperfect gas theory,<sup>6</sup> the second virial coefficient can be generally written as

$$B_2 = -\frac{1}{2} \left[ \int \{e^{-\beta u(r)} - 1\} d\bar{r} \right] = -\frac{1}{2} \left[ \int f d\bar{r} \right] \quad (2)$$

where  $1/\beta$  is the multiple of the Boltzmann constant  $k$  and temperature. The Mayer  $f$  function replaces the integrand in eq 2. When a functional form of the interparticle potential  $u(r)$  is chosen, the required molecular parameters of  $u(r)$  are determined from comparison of the experimental  $B_2$  with the theoretical one in eq 2. A good choice of parameters should give a good representation of the experimental  $B_2$ . Once these parameters for  $u(r)$  are determined, they can be used to regenerate any part of integral in eq 2.

For our 2nd lattice,  $B_2$  is rewritten in a discretized form by separating the integral into the subintegrals for each lattice cell and regrouping them for each neighbor:

$$\begin{aligned} B_2 = & -\frac{1}{2} \left[ - \int_{\text{cell}} d\bar{r} + \sum_{1\text{st}} \int_{\text{cell}} f d\bar{r} + \right. \\ & \left. \sum_{2\text{nd}} \int_{\text{cell}} f d\bar{r} + \sum_{3\text{rd}} \int_{\text{cell}} f d\bar{r} \dots \right] \\ = & \frac{V_c}{2} \left[ 1 - \sum_{1\text{st}} \langle f \rangle_{1\text{st}} - \sum_{2\text{nd}} \langle f \rangle_{2\text{nd}} - \sum_{3\text{rd}} \langle f \rangle_{3\text{rd}} - \dots \right] \quad (3) \end{aligned}$$

where the volume element  $\int_{\text{cell}} d\bar{r}$  is the volume  $V_c$  of one lattice cell of the 2nd lattice. In the second expression in eq 3,  $V_c$  has been taken out of the bracket with the introduction of a cell average Mayer function,  $\langle f \rangle$ . It is natural from eq 3 to define the cell average  $\langle f \rangle$  as

$$\langle f \rangle = \int_{\text{cell}} f d\bar{r} / \int_{\text{cell}} d\bar{r} \quad (4)$$

In the calculation of the cell average  $\langle f \rangle$ , the center of one monomer, if the other is fixed at the origin, is

**Table 1. The Average Mayer Functions and the Converted Effective Interaction Parameters for the Indicated Shell Vectors ( $T = 443$  K)**

shell	selected vector	no. of spherically equivalent vectors	average Mayer $f$ function	overall shell average $f$ function	effective interaction parameter (kJ/mol)
1	(1, -1, 0)	6	-0.9997	-0.9664	12.5008
	(1, 0, 0)	6	-0.9331		
2	(1, -1, 1)	6	-0.5969	-0.0226	0.0842
	(1, 1, 0)	6	-0.1261		
	(2, -1, 0)	12	-0.0363		
	(2, -1, -1)	6	0.0959		
	(2, 0, 0)	6	0.1661		
	(2, -2, 0)	6	0.3754		
3	(2, -2, 1)	12	0.3131	0.1805	-0.6112
	(2, 1, -1)	12	0.2854		
	(3, -1, -1)	6	0.2087		
	(1, 1, 1)	2	0.2029		
	(2, 1, 0)	12	0.1680		
	(3, -1, 0)	12	0.1474		
	(3, 0, -2)	12	0.1337		
	(3, -2, -1)	12	0.1297		
	(3, 0, 0)	6	0.0757		
	(3, -3, 0)	6	0.0613		
4		162 <sup>a</sup>		0.0379	-0.1371
5		252 <sup>a</sup>		0.0097	-0.0356

<sup>a</sup> For the fourth and fifth shells, only the total number of neighbor vectors (or coordination numbers) are shown in this table. <sup>b</sup> The employed L-J parameters are  $\epsilon/k = 205$  K,  $\sigma = 4.2$  Å.

allowed to be anywhere in the given lattice cell. Equation 3 is further manipulated to give

$$B_2 = \frac{V_c}{2} [1 - z_1 \bar{f}_{1st} - z_2 \bar{f}_{2nd} - z_3 \bar{f}_{3rd} - \dots] \quad (5)$$

where  $z_i$  is the coordination number of the  $i$ th nearest neighbor. The first through fifth coordination numbers of the 2nd lattice are 12, 42, 92, 162, and 252, respectively. In eq 5, the overall average Mayer function,  $\bar{f}_{th}$ , for the  $i$ th neighbor is the arithmetic mean of  $\langle f \rangle$ 's. Finally the effective interaction parameter,  $u_i$ , representing the  $i$ th neighbor, is defined as

$$e^{-\beta u_i} - 1 \equiv \bar{f}_{th} \quad (6)$$

Only one interaction parameter is applied to a given nearest neighbor.

The  $B_2$  for polymer systems, due to the connectivity, needs a minor correction to eq 2:

$$B_2 = -\frac{1}{2} \sum_k \sum_l \int \{e^{-\beta u_{kl}(r)} - 1\} d\mathbf{r} + \xi \quad (7)$$

where  $u_{kl}$  implies the mer-mer potential invoked by the  $k$ th and the  $l$ th monomers on two chains. The additional term  $\xi$  arises from a mixed inter-intramolecular interaction between two mers on one chain and another mer on a different chain.<sup>7</sup> Since the first term in eq 7 is dominant as chains become longer,<sup>8</sup> we ignore  $\xi$  and use eq 5 for  $B_2$  per one interaction pair for polymer systems.

In our previous communication, we suggested a scheme (method 1) to estimate the interaction parameter,  $u_i$  from the vanishing  $B_2$  at the  $\Theta$  condition.<sup>4,5</sup> This method does not provide a unique set of interaction parameters. Infinitely many sets of parameters would satisfy the condition that  $B_2 = 0$ . In addition to this aspect, we have to measure the interaction parameters at the yet unknown  $\Theta$  temperature. To simplify this problem, only the first two neighbor interactions,  $u_1$  and  $u_2$ , were considered. The first neighbor parameter  $u_1$

would be positive to represent the repulsion. As a counteraction, the second parameter  $u_2$  must be negative. Assuming that  $\Theta = 300$  K, the set of parameters that simulate the unperturbed dimension of a 2nd chain was determined. The obtained parameters were  $u_1 = 0.6$  kJ/mol and  $u_2 = -0.2$  kJ/mol.

Our new and alternative scheme (method 2) is the direct evaluation of the subintegrals in eq 3 by using a known potential energy function. Assume that the system has only two monomers. Equation 5 then applies. To estimate the individual  $\bar{f}_{th}$  or  $u_i$ , a commonly used interparticle potential, such as the Lennard-Jones (L-J) potential, is employed and integrated to obtain  $\langle f \rangle$  as described for eq 6. Once we know the L-J potential parameters of monomeric units, we can easily calculate the effective interactive parameters  $u_i$ 's. The reasonable range of parameters can at least be estimated in this way. Instead of using the soft core potential, the truncated L-J potential in eq 8 with hard core is used to ensure the volume exclusion.

$$u = \begin{cases} \text{hard} & r < 2.5 \text{ Å} \\ u_{L-J} = 4\epsilon \left[ \left( \frac{\sigma}{r} \right)^{12} - \left( \frac{\sigma}{r} \right)^6 \right] & r > 2.5 \text{ Å} \end{cases} \quad (8)$$

The two associated parameters,  $\epsilon$  and  $\sigma$ , for a given monomer should be optimized to have the best fit to certain selected properties. For a priori estimation of the effective 2nd lattice parameters, however,  $\epsilon$  and  $\sigma$  of  $\text{CH}_2=\text{CH}_2$  ( $\epsilon/k = 205$  K,  $\sigma = 4.2$  Å)<sup>9</sup> are used instead of the unknown values for  $-\text{CH}_2\text{CH}_2-$  as a segment of a long chain. With this pair of L-J parameters, use of eq 5 up to the fifth neighbor shell gives  $B_2/(\text{Å})^3 = -64.47$  at 443 K, whereas direct calculation via eq 2 gives  $B_2/(\text{Å})^3 = -57.5$  (cutoff at 10 Å) to  $-67.89$  (cutoff at 12.5 Å). We also report a few results for simulations with slightly different  $\epsilon$  or  $\sigma$ , in order to determine the sensitivity to minor adjustments in these parameters. The L-J parameters employed should not exceed those of  $\text{CH}_3-\text{CH}_3$  ( $\epsilon/k = 230$  K,  $\sigma = 4.4$  Å).<sup>9</sup>

Tables 1 and 2 show the estimated  $u_i$ 's for the first five nearest neighbors (or coordination shells in the

**Table 2. The Average Mayer Functions and the Converted Effective Interaction Parameters for the Indicated Shell Vectors ( $T = 370$  K)**

shell	selected vector	no. of spherically equivalent vectors	average Mayer $f$ function	overall shell average $f$ function	effective interaction parameter (kJ/mol)
1	(1,-1,0)	6	-0.9999	-0.9666	10.4583
	(1,0,0)	6	-0.9334		
2	(1,-1,1)	6	-0.5830	0.0357	-0.1079
	(1,1,0)	6	-0.0762		
	(2,-1,0)	12	0.0197		
	(2,-1,-1)	6	0.1661		
	(2,0,0)	6	0.2333		
	(2,-2,0)	6	0.4704		
3	(2,-2,1)	12	0.3876	0.2220	-0.6168
	(2,1,-1)	12	0.3552		
	(3,-1,-1)	6	0.2560		
	(1,1,1)	2	0.2537		
	(2,1,0)	12	0.2063		
	(3,-1,0)	12	0.1799		
	(3,0,-2)	12	0.1626		
	(3,-2,-1)	12	0.1577		
	(3,0,0)	6	0.0916		
	(3,-3,0)	6	0.0739		
4		162 <sup>a</sup>		0.0457	-0.1375
5		252 <sup>a</sup>		0.0116	-0.0356

<sup>a</sup> For the fourth and fifth shells, only the total number of neighbor vectors (or coordination numbers) are shown in this table. <sup>b</sup> The employed L-J parameters are  $\epsilon/k = 205$  K,  $\sigma = 4.2$  Å.

spherical sense) at 443 and 370 K. For the first three neighbors, some of the cell vectors are specifically tabulated in the second column. In the next column, the number of spherically equivalent vectors implies the number of pointing vectors of the given neighbor that have the same average Mayer function due to the spherical symmetry. The arithmetic average Mayer function and the effective interaction parameters are then calculated. For simplicity, the first three interaction parameters only are employed in the equilibration of the systems in the simulations. For the fourth and fifth shells, only the final average Mayer functions and interaction parameters are tabulated in these tables. The temperature dependence of the interaction parameters is unavoidable, since the calculation is performed at a single point of  $B_2$ . An optimization scheme over several temperatures may reduce the dependence of  $u_i$ 's on temperature. It is also shown from these tables that repulsion becomes more important as temperature increases.

As can be seen in these tables, the interaction parameter for the second neighbor is small, and not apparently negative. The small  $u_2$  is due to the fact that the second nearest neighbor of the 2nd lattice covers from 2.5–5 Å. The collision diameter  $\sigma$  of ethylene is 4.2 Å. The repulsion and the attraction are averaged out in the second neighbor. Therefore the attractive third neighbor is necessary for the cohesion of polyethylene chains. The higher neighbor interactions are also attractive, but more weakly so than the third neighbor. In Figure 2, the L-J potential is plotted as a function of the scaled intermer distance  $r/\sigma$ . The 2nd lattice interaction parameters are overlaid on this figure. The length of each line implies the intermer distance region that is covered by the corresponding shell.

In Table 3, the additional sets of the 2nd lattice interaction parameters are evaluated by using the two variants of the L-J parameters for ethylene. These lattice parameters will also be used for the simulation to investigate the dependence of simulated nonbonded energies and cohesive energies on the various sets of the L-J parameters.

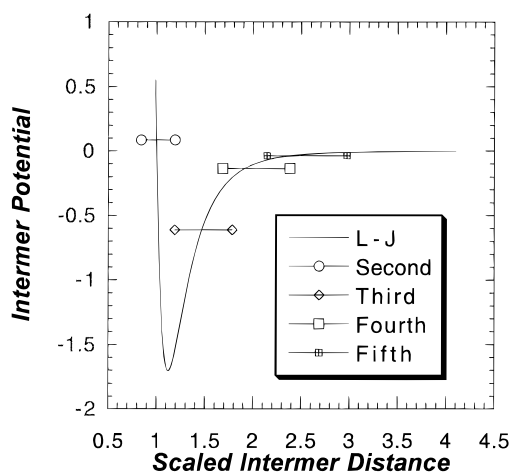


**Figure 2.** The 2nd lattice interaction potential at 443 K and the Lennard-Jones (L-J) potential in kilojoules/mole as functions of the scaled intermer distance  $r/\sigma$ , where  $\epsilon/k = 205$  K and  $\sigma = 4.2$  Å for the L-J potential. The 2nd lattice potential is a step function. The vertical position of each horizontal line, end-blocked with symbols, for the indicated 2nd neighbor shell represents the effective interaction parameter. Its length implies the range of the distance of the neighbor shell vectors from the origin.

**Table 3. The Interaction Parameters Representing the Indicated Neighbor Shells for Various Sets of the L-J Parameters ( $T = 443$  K)**

shell	$u_k$ (kJ/mol)	
	$\epsilon/k = 185$ K, $\sigma = 4.2$ Å	$\epsilon/k = 205$ K, $\sigma = 4.4$ Å
1	12.3654	14.2146
2	0.1660	0.4288
3	-0.5443	-0.6985
4	-0.1219	-0.1722
5	-0.0316	-0.0449

The two methods suggested here incorporate not a lattice potential with hard core attraction, but a potential with hard core-finite repulsion-attraction. It will be shown later that this three way potential yields a unique nonbonded energy-density relationship.

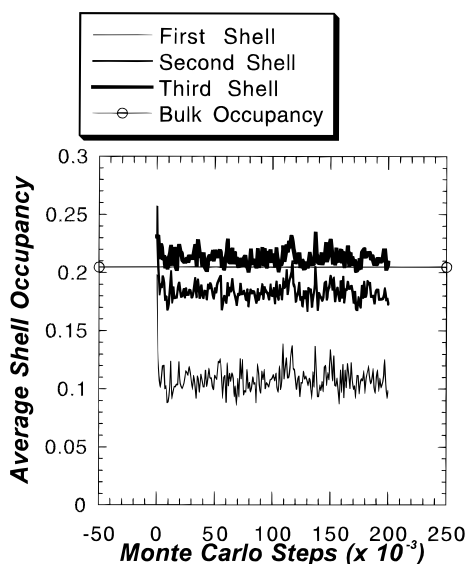


**Figure 3.** The average neighbor shell occupancies of the system at the density of  $0.853 \text{ g/cm}^3$ . Input interaction parameters are  $u_1 = 0.6 \text{ kJ/mol}$ , and  $u_2 = -0.2 \text{ kJ/mol}$  (method 1). The straight line, end-blocked with open circles, indicates the bulk occupancy (0.205).

### System Description

Our model system consists of 5–15 chains of  $[-\text{CH}_2-\text{CH}_2-]_{50}$  (50-mer in the 2nd lattice viewpoint) on a  $13 \times 13 \times 13$  lattice box with the conventional periodic boundary condition. A long-chain system is necessary to avoid evaporation. The densities of the system cover from 0.47 to  $1.4 \text{ g/cm}^3$ , within which the density of liquid PE mostly falls.

We run only a small number of Monte Carlo Steps up to 200 000 for the average cell occupancy of nearest neighbors and the nonbonded energy calculation, with inclusion of the long-range interaction. The Monte Carlo procedure itself has been described previously in detail.<sup>4</sup> Each fundamental move changes the coordinates of one bead only, by moving it to a vacant nearest-neighbor site. Soon after the plateau of the average neighbor occupation is reached, the earlier part of the simulation is discarded in the calculation of the average occupation and then energy. The system temperature is set to 443 K ( $170^\circ\text{C}$ ), well above the melting point of PE. Temperature, however, is not an important factor in the energy calculation, since the energy is mainly an implicit function of temperature.

### Average Occupancy of Several Nearest Neighbors

The physical properties of polymer chains in the multichain system at bulk density converge to their equilibrium values at very different rates, depending on the properties. For a feasible test of chosen interaction parameters, rapidly equilibrating properties, yet relatively independent of chain relaxation, are desired. The average occupancy of the first several nearest neighbors by nonbonded monomers has been shown to rapidly converge to a stable value, as can be seen in Figures 3 and 4 for two different methods. The input cell occupancy of the systems in these figures is 0.205 (9 chains in  $13 \times 13 \times 13$  box, or a density of  $0.85 \text{ g/cm}^3$ ). The equilibrium occupancy of the first shell is much smaller than 0.205, as expected from the large positive value of  $u_1$ . In contrast, the occupancy of the third shell is only slightly greater than 0.205 (by 6%). This

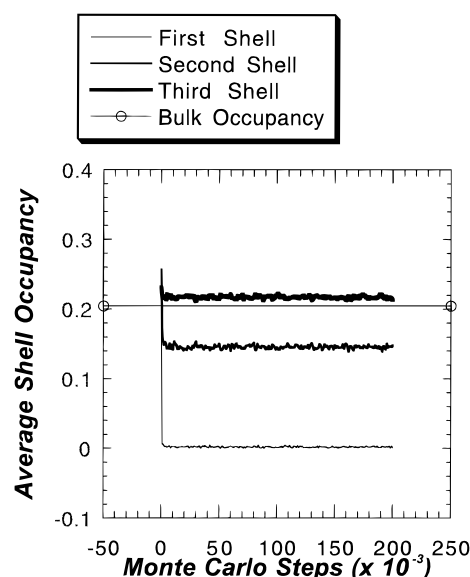


**Figure 4.** The average neighbor shell occupancies of the system at the density of  $0.853 \text{ g/cm}^3$ . Input interaction parameters were obtained by using the L-J potential parameters ( $\epsilon/k = 205 \text{ K}$ , and  $\sigma = 4.2 \text{ \AA}$ ; method 2). The straight line, end-block with open circles, indicates the bulk occupancy (0.205).

**Table 4. The Average Numbers of Sites Occupied by Nonbonded Monomers (Method 1)<sup>a</sup>**

density ( $\text{g/cm}^3$ )	shell		
	1	2	3
0.474	0.682	4.464	11.921
0.664	0.975	6.036	15.733
0.853	1.299	7.695	19.545
1.043	1.645	9.406	23.534
1.233	2.028	11.180	27.625
1.422	2.429	12.976	31.631

<sup>a</sup> The employed parameters are  $u_1 = 0.6 \text{ kJ/mol}$  and  $u_2 = -0.2 \text{ kJ/mol}$  at  $T = 300 \text{ K}$ .

**Table 5. The Average Numbers of Sites Occupied by Nonbonded Monomers (Method 2)<sup>a</sup>**

density ( $\text{g/cm}^3$ )	shell		
	1	2	3
0.474	0.009	3.667	13.903
0.664	0.010	4.196	16.251
0.853	0.023	6.135	20.037
1.043	0.068	8.759	23.643
1.233	0.234	11.339	27.330
1.422	0.586	13.654	31.353

<sup>a</sup> The employed L-J parameters are  $\epsilon/k = 205 \text{ K}$ ,  $\sigma = 4.2 \text{ \AA}$ . The 2nd lattice interaction parameters are estimated at  $T = 443 \text{ K}$ .

difference between the shell occupancy and the bulk occupancy is gradually diminishing (3% for the fourth shell, and 0.8% for the fifth shell).

It should be pointed out that monomers on one chain, separated by three or more 2nd bonds, are counted in the calculation of the average nonbonded occupancy. The purpose of the occupancy estimation is the calculation of the long-range or nonbonded interaction. The interaction between monomers separated by two bonds is already considered in the short-range interaction.<sup>4</sup>

Tables 4 and 5 show the average numbers of lattice sites occupied by the nonbonded monomers up to the third nearest neighbors from the simulations (methods 1 and 2, respectively). The relatively weak repulsion ( $u_1 = 0.6 \text{ kJ/mol}$ ) in method 1 allows slightly more than one nonbonded monomer to penetrate into the first

neighbor shell. In method 2, the first neighbor is mostly avoided due to the strong repulsion ( $u_1 = 12.5$  kJ/mol) put into the system. Meanwhile, the occupancies of the second and third neighbors are only slightly different in both cases, particularly at the higher densities. The number of monomers in these two neighbors is mostly determined by the input density. The successive motion for chain relaxation does not appear to change the average neighbor occupancy significantly.

### Nonbonded Energy and Cohesive Energy

We probe systems with densities from 0.47 to 1.4 g/cm<sup>3</sup>. All higher densities, we may face the partial alignments of chains after long runs. At lower densities, in contrast, the system may be in the region of the negative pressure. This negative pressure may cause a vacuum inside the system. Regardless of all these difficulties, we persist in this nonbonded energy calculation to have an insight into the primary effect of input interaction parameters.

The average nonbonded cell occupancies obtained above are used to calculate the long-range interaction. This nonbonded energy gives a stringent test for the chosen interaction parameter pair. With a very dilute gas as the starting point, the nonbonded energy of the system decreases as density increases. However, the energy should pass through a minimum at a certain density. As density becomes larger than this point, the repulsion between nonbonded monomers in the system starts to prevail. This repulsion results in the increase of the nonbonded energy. This statement of the minimum energy is neither generally recognized nor easily obtainable. The van der Waals type of interaction does not possess this property unless the space is completely filled with chains leaving no free volume. This is probably the reason that the monotonic decrease of the energy is commonly believed.

Recently, Cho and Sanchez pointed out this minimum energy by showing that the volume derivative of the energy, or the internal pressure, has a maximum.<sup>10–12</sup> The maximum internal pressure occurs at the inflection point of the energy. After passing through the inflection point, the energy changes its shape to reach the minimum and eventually go to infinity. Its shape resembles that of the interparticle potential. In comparison, the van der Waals type of energy does not have this inflection point of the energy. It reaches the minimum energy monotonically and jumps to infinity. A simple lattice potential with hard core–attractive interaction generally yields the van der Waals energy.

The nonbonded long-range energy was first calculated by using the lattice interaction parameters and Table 4 for method 1, and plotted as a function of density in Figure 5. The nonbonded energy appears to be monotonically decreasing. This is somewhat misleading, because method 1 yields the minimum energy at a density around 3 g/cm<sup>3</sup> (results not depicted here). However, this density at the minimum energy is aphysical. The simulated nonbonded energies are also small in magnitude. Even though the parameters enable the model chain to have the  $\Theta$  dimension, the weak nonbonded energy and the aphysical density of the minimum energy suggest (1) the weak repulsion largely underestimates the physical existence of the monomeric unit ( $-\text{CH}_2\text{CH}_2-$ ) on the 2nd lattice ( $\sigma = 4.2$  Å, while one lattice spacing on the 2nd lattice is 2.5 Å), (2) placing all of the attraction in the attractive

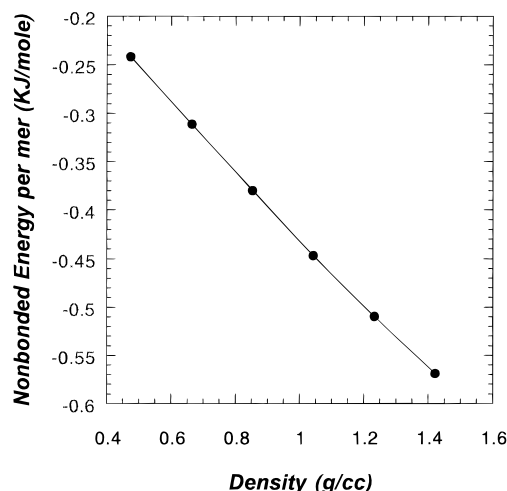


**Figure 5.** The nonbonded energy per monomer as a function of density. The 2nd lattice interaction parameters are the same that were used for Figure 3.

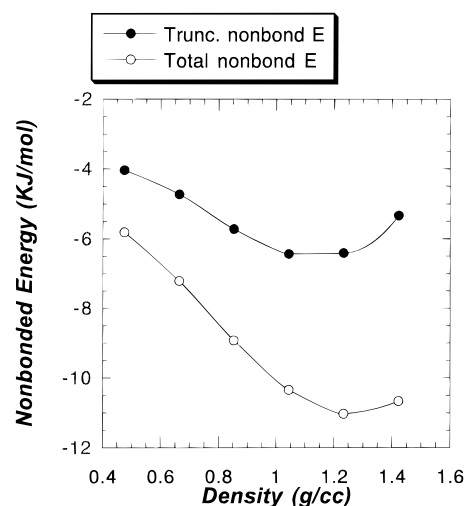


**Figure 6.** The nonbonded energy per monomer as a function of density. The 2nd lattice interaction parameters are those used for Figure 4. The minimum of the nonbonded energy is apparently shown at the density around 1.2 g/cm<sup>3</sup>.

second neighbor interaction enhances the aphysical cohesion of the system.

The nonbonded energy is calculated by using the lattice interaction parameters and Table 5 for method 2 as our second test. As was mentioned before, the simulations in method 2 were performed with only the first three interaction parameters. This implies that the cutoff distance of the interparticle potential is 7.5 Å. The attractive cutoff energy, which originates in the higher shell contribution, should be calculated. One can estimate the average occupancies of higher shells from the uncorrelated bulk lattice occupancy, since these two occupancies do not differ appreciably. Figure 6 shows the nonbonded energy and density relationship for method 2. As is seen in this figure, the energy has a minimum at a density around 1.2 g/cm<sup>3</sup>. The density of minimum energy is now in a physically reasonable range. The undesirable features regarding method 1, which were mentioned above, are corrected in method 2 to a certain degree. The first neighbor is more strongly repulsive, and the principal source of attraction is moved from the second to the third neighbor. Therefore, the system can avoid a further cohesion before reaching an aphysical density.

**Table 6. The Additional Data of Nonbonded Energies of the System at the Density of 0.853 g/cm<sup>3</sup> with the Indicated Sets of the L-J Parameters**

energy (kJ/mol) parameters	simulated energy	cut-off energy	total
$\epsilon/k = 185 \text{ K}, \sigma = 4.2 \text{ \AA}$	-4.784	-2.841	-7.625
$\epsilon/k = 205 \text{ K}, \sigma = 4.4 \text{ \AA}$	-5.817	-4.016	-9.833

**Table 7. Number of Nonbonded Contacts of a Single Chain to the Indicated Neighbor Shells for Various Sets of the L-J Parameters, and the Energy Arising from the Total**

shell	occupied sites		
	$\epsilon/k = 185 \text{ K}$ $\sigma = 4.2 \text{ \AA}$	$\epsilon/k = 205 \text{ K}$ $\sigma = 4.2 \text{ \AA}$	$\epsilon/k = 205 \text{ K}$ $\sigma = 4.4 \text{ \AA}$
1	0.004	0.004	0.002
2	1.214	1.271	1.160
3	4.754	4.882	4.851
4	5.557	5.657	5.493
5	6.596	6.686	6.517
total	18.125	18.500	18.023
$E \text{ (kJ/mol)}$	-1.610	-1.921	-2.047

**Table 8. The Calculated Cohesive Energies per Monomer for the Three Sets of the L-J Parameters**

	parameter set		
	$\epsilon/k = 185 \text{ K}$ $\sigma = 4.2 \text{ \AA}$	$\epsilon/k = 205 \text{ K}$ $\sigma = 4.2 \text{ \AA}$	$\epsilon/k = 205 \text{ K}$ $\sigma = 4.4 \text{ \AA}$
cohesive energy per monomer (kJ/mol)	6.015	6.996	7.786

The existence of the minimum energy in our simulation originates from the incorporation of the hard core, the finite repulsive interaction, and the attractive interaction parameters. Without the finite repulsive interaction, we can only experience the increase of the cohesion with the increase of density, as the van der Waals fluid does.

The long-range energy measured from the simulation directly gives the so-called cohesive energy (CE). This energy can be equated to

$$\text{CE} = \{N_c \times \text{single chain total energy}\} - \{\text{total energy of multichain system}\} \quad (9)$$

where  $N_c$  is the number of chains in the system. The first term in eq 9 is the system energy at infinite dilution. The total short-range energy is approximately the same in a dense or a dilute system. Therefore, the CE is equated to the difference between the intramolecular and the intermolecular nonbonded energies. We already calculated and plotted the nonbonded energy of the bulk system in Figure 6. The density of the system is fixed at 0.853 g/cm<sup>3</sup>, which is close to the density of amorphous polyethylene at room temperature. In Table 6, the additional nonbonded energy data at the density of 0.853 g/cm<sup>3</sup> are presented for the system with other sets of the L-J parameters. The intramolecular nonbonded energy can be obtained by probing the nonbonded contacts of an arbitrarily chosen chain (in the bulk) with itself and then averaging over all chains. Table 7 shows the measured nonbonded contacts of a chain in the simulated system with the three sets of the L-J parameters. These contact numbers or the number of occupied sites are then used to calculate the average intramolecular nonbonded energy. As is seen in Table 8, the simulation yields the CE = 6.0–7.8 kJ/mol for the three cases. Meanwhile, the

experimental cohesive energy at room temperature, which is the square of the solubility parameter, is 8–9 kJ/mol.<sup>13</sup> Therefore, the simulated CE is in qualitative agreement with the experiment for the three trials of the lattice interaction parameters. The results in Table 8 suggests that either a deeper potential well (larger  $\epsilon$ ) or stronger volume exclusion (larger  $\sigma$ ) yields a larger CE. It is also expected that the L-J parameters between those of CH<sub>2</sub>=CH<sub>2</sub> ( $\epsilon/k = 205 \text{ K}, \sigma = 4.2 \text{ \AA}$ ) and those of CH<sub>3</sub>–CH<sub>3</sub> ( $\epsilon/k = 230 \text{ K}, \sigma = 4.4 \text{ \AA}$ ) would simulate the CE in the known experimental range.

It should be pointed out that the cohesive energy estimation may be enhanced without the further manipulation of the interaction parameters. When the shell average interaction parameters were estimated, the arithmetic mean of equally weighted cell averaged Mayer functions yielded the representative interaction parameter for the given neighbor shell. For nonbonded contacts in a given neighbor shell, there is no preference of lattice points on which monomers are placed. In the continuum space, these nonbonded contacts can move preferentially toward more attractive regions of the potential well, which will increase the CE.

In summary, the suggested interaction parameters (method 2) show a desired qualitative feature of the nonbonded energy with a minimum at a physical density. The simulated cohesive energy is in qualitative agreement with the experimental value for the chosen trials of interaction parameters. The results suggest that a careful selection of the excluded volume effect and the attraction (or  $\sigma$  and  $\epsilon$ ) could give a close prediction of the cohesive energy. The selected  $\sigma$  and  $\epsilon$ , however, should not push the system to have the minimum nonbonded energy at higher densities.

## Conclusions

A high coordination (2nnd) lattice simulation of coarse-grained RIS polyethylene chains is visited here. For the simulation of the realistic behavior of polyethylene, the cohesion in the system is considered. A long-range interaction between nonbonded monomers gives a dominant contribution to system cohesion. The second virial coefficient  $B_2$  in a continuous space was suitably discretized for the 2nnd lattice. Two methods were suggested to estimate the long-range interaction parameters, in addition to the hard core, for several nearest neighbors: (1) two-parameter potential that makes the  $B_2$  of an isolated chain vanish at  $\Theta$  temperature; (2) three-parameter potential obtained from the direct integration of the Mayer function in the expression of  $B_2$  using the Lennard-Jones potential. The model potential for the 2nnd lattice is more general than a simple square-well potential. We include a hard core, a finite repulsive interaction, and an attractive interaction.

As a first and relatively simple test, the average occupancy of first several nearest neighbors and the corresponding nonbonded energy were measured from the 2nnd lattice simulation of polyethylene of DP 50. We observed that the calculated nonbonded energy as a function of density has a minimum in our two suggested methods. This minimum energy is not generally seen in the van der Waals fluid. Method 2 yields the minimum energy at density around 1.2 g/cm<sup>3</sup>. The system with the two interaction parameters from the vanishing  $B_2$  was shown to have the minimum energy at an aphysical density. This result suggests that the three-parameter lattice potential from the direct inte-

gration with the L-J potential better describes the interaction between nonbonded monomers on the 2nd lattice. The cohesive energy was also calculated from the obtained nonbonded energy. The cohesive energy from the simulation was in qualitative agreement with the experimental value.

A reasonable estimation of interaction parameters for the 2nd lattice should result in proper measurements of physical properties of polymers. Our successive efforts on the 2nd simulation of polymers will be continued to simulate chain dimensions in the bulk and to measure pressure and surface tension. The suggested scheme will also be applied to other homopolymer and block copolymer systems.

**Acknowledgment.** This work was supported by National Science Foundation Grant DMR 9523278.

## References and Notes

- (1) Flory, P. J. *Statistical Mechanics of Chain Molecules*; Wiley: New York, 1969.
- (2) Mattice, W. L.; Suter, U. W. *Conformational Theory of Large Molecules. The Rotational Isomeric State Model in Macromolecular Systems*; Wiley: New York, 1994.
- (3) Rapold, R. F.; Mattice, W. L. *J. Chem. Soc., Faraday Trans.* **1995**, *91*, 2435.
- (4) Rapold, R. F.; Mattice, W. L. *Macromolecules* **1996**, *29*, 2457.
- (5) Doruker, P.; Rapold, R. F.; Mattice, W. L. *J. Chem. Phys.* **1996**, *104*, 8742.
- (6) McQuarrie, D. A. *Statistical Mechanics*; Harper & Row: New York, 1976.
- (7) Honnel, K. G.; Hall, C. K.; Dickmann, R. *J. Chem. Phys.* **1987**, *87*, 664.
- (8) Schweizer, K.; Curro, J. G. *J. Chem. Phys.* **1988**, *89*, 3342.
- (9) Hirschfelder, J. O.; Curtiss, C. F.; Bird, B. B. *Molecular Theory of Gases and Liquids*; Wiley: New York, 1954.
- (10) Sanchez, I. C.; Cho, J. *Polymer* **1995**, *36*, 2929.
- (11) Cho, J. Ph.D. Dissertation at the University of Texas at Austin, 1995.
- (12) Cho, J.; Sanchez, I. C. Manuscript in preparation.
- (13) van Krevelen, D. W. *Properties of Polymers*; Elsevier Science Publishers B. V.: Amsterdam, Netherlands, 1990.

MA961287G